Pergamon

*Polyhedron* Vol. 16, No. 21, pp. 3815–3826, 1997
© 1997 Elsevier Science Ltd
All rights reserved. Printed in Great Britain
0277–5387/97 $17.00+0.00

PII: S0277–5387(97)00143–5

# Copper(II) complexes of optically active binucleating ligands, N,N′-bis[2-pyridylmethyl and 2-(2-pyridyl)ethyl]-(S)-malamide and related amides

Kiyoko Nonoyama,[a]* Wasuke Mori,[b] Kiyohiko Nakajima[c] and Matsuo Nonoyama[d]

[a] Konan Junior College, Takaya-cho, Konan, Aichi 483, Japan

[b] Department of Chemistry, Faculty of Science, Kanagawa University, Tsuchiya, Hiratsuka, Kanagawa 259-12, Japan

[c] Department of Chemistry, Aichi University of Education, Igaya, Kariya, Aichi 448, Japan

[d] Department of Chemistry, Faculty of Science, Nagoya University, Chikusa, Nagoya 464, Japan

(Received 4 February 1997; accepted 7 April 1997)

**Abstract**—N,N′-Bis(2-pyridylmethyl)-3-hydroxyglutaramide [abbreviated as $H_3$(pmg)], optically active N,N′-bis{2-pyridylmethyl and 2-(2-pyridyl)ethyl}-(S)-malamide [$H_3$(lpm) and $H_3$(lpe), respectively], and the optically inactive analogues [$H_3$(ppm) and $H_3$(pem)] gave dimeric copper(II) complexes [$Cu_2XL$]·n$H_2O$ (L = lpm, lpe, pmm, pem, and pmg; X = an anionic, *exo*-bridging ligand such as chloride, hydroxide, acetate (OAc), pyrazolate (pz), and nitrite ions). These complexes were characterized by magnetic susceptibilities, and electronic, circular dichroism, and infrared spectra. The amides act as a trivalent anionic ligand coordinating through the pyridine- and deprotonated amido-nitrogen atoms and through the deprotonated, pendant alkoxo-oxygen atom bridging two copper ions. Many of the complexes were magnetically subnormal at room temperature, the magnetic interaction between the two copper ions depending upon both L and the *exo*-bridges, X. The antiferromagnetic interaction increased in the order of X, Cl < OAc < OH < $NO_2$ < pz. Temperature dependence of the magnetic susceptibilities of some of the lpm complexes ensured the order. A diamagnetic nickel(II) complex, $Ni_2$(pz)(lpm)·2$H_2O$ and a heterometallic CuNi(pz)(lpm)·2$H_2O$ were also obtained. The binuclear structure of $Cu_2$(pz)(ppm)·3$H_2O$ was confirmed by X-ray analysis. © 1997 Elsevier Science Ltd

*Keywords*: copper(II) complexes; binucleating ligands; optically active complexes; acid amide derivatives; X-ray analysis; antiferromagnetic interaction.

There are many studies of antiferromagnetically coupled, binuclear copper(II) complexes in context with approach to mimicking the active sites of the type III dinuclear copper enzymes [1]. One class of ligands forming such binuclear copper(II) complexes well studied are binucleating Schiff bases with pendant alcohol (or phenol) groups, the deprotonated oxygen atoms acting as bridging donors (Fig. 1). It seems appropriate to substitute acid amide groups for the imine groups of the Schiff bases, because proteins consist of amino acids combined by acid amide (peptide) groups. There are, however, little studies on complexes of binucleating acid amide derivatives [2], which may provide us with more realistic model systems than Schiff base ligands. Continuing our studies

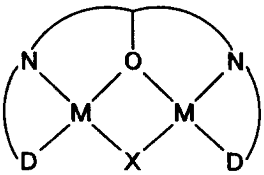

Fig. 1. Diagrammatic representation of a binuclear complex. "D" represents a terminal donor, "M" a central metal, and "X" an *exo*-bridging ligand. The charge of the complex is out of consideration.

---

* Author to whom correspondence should be addressed.

on binuclear copper(II) complexes of acid amide derivatives [3], we have investigated copper(II) complexes of hydroxy group-functionalized, N,N′-disubstituted diacid amides as ligands possessing a similar frame to that of the Schiff's bases mentioned above (Fig. 2). The new amides used are abbreviated as follows: N,N′-bis(2-pyridylmethyl)-3-hydroxyglutaramide as $H_3$(pmg), optically active N,N′-bis[2-pyridylmethyl and 2-(2-pyridyl)ethyl]-(S)-malamide, respectively, as $H_3$(lpm) and $H_3$(lpe), and the racemic analogues, respectively, as $H_3$(ppm) and $H_3$(pem). $H_3$(lpm) and $H_3$(lpe) derived from natural (S)-(–)-malic acid seem to be a rare example of optically active binucleating ligands providing complexes with the frame of Fig. 1.

## RESULTS AND DISCUSSION

The amide ligands (Fig. 2) were prepared by the reaction of 2-aminomethylpyridine or 2-(2-aminoethyl)pyridine with dimethyl-(S)-(–)-malate, dimethyl 3-hydroxyglutarate, or diethyl (RS)-malate on an oil bath (130°C) for 3 h. $H_3$(pmg) and $H_3$(pem) crystallized in white free form but $H_3$(pmm) and $H_3$(lpm) could be isolated as colorless sulfates. $H_3$(lpe) remained as an oil after several attempts of crystallization and the amide was, therefore, used without isolation. The IR spectra shows the characteristic bands of secondary amides [4]: the amide I bands between 1675–1636 $cm^{-1}$ and the amide II bands between 1520–1567 $cm^{-1}$. The region 3000–3500 $cm^{-1}$ are complicated and an unambiguous assignment of $\nu$(NH) and $\nu$(OH) is impossible. $^1H$ and $^{13}C\{^1H\}$ NMR spectra also provided the evidence for the formation of the expected amides. The two pyridylmethyl (and -ethyl) carbamoyl moieties of malamides are not equivalent and the NMR spectra are complicated but the two moieties of 3-hydroxyglutaramide are equivalent and the spectra are rather simple. The characteristic $^{13}C$ signal of an amide group (CONH) was observed in the range 169–175 ppm. Although $H_3$(lpe) was not isolated, the IR and NMR spectra proved the formation of the desired compound without doubt.

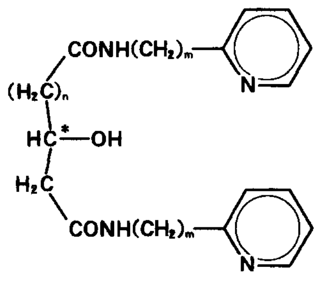

$H_3$(lpm) ; m = 1, n = 0, * = (S)

$H_3$(pmm) ; m = 1, n = 0, * = (R S)

$H_3$(lpe) ; m = 2, n = 0, * = (S)

$H_3$(pem) ; m = 2, n = 0, * = (R S)

$H_3$(pmg) ; m = 1, n = 1

Fig. 2. Binucleating acid amide ligands with a hydroxy pendant group and their abbreviations. "R" and "S" represent a chirality of an asymmetric carbon.

Under basic condition, the ligands ($H_3L$) reacted with copper(II) salt (1 : 2 molar ratio) to form complexes of a general composition, $Cu_2(OH)L \cdot nH_2O$, where L is anionic trivalent (Table 1). The OH group could be replaced with other mono anionic ligands under appropriate conditions and the products with satisfactory analytical results are given in Table 1. Pyrazolato (pz) complexes were obtained most easily. Formation of corresponding nickel(II) complexes was severely limited and only two pz complexes were acquired. Heterometallic complexes, CuNi(pz)L $\cdot nH_2O$ (L = lpm, $n$ = 2 and L = pmm, $n$ = 5), were also obtained.

The dimeric structure (Fig. 3) of $Cu_2$(pz)(pmm)$\cdot$ $3H_2O$ has been confirmed by X-ray analysis and is shown in Fig. 4 with atom labelling scheme. The bond distances and angles are summarized in Table 2. The three water molecules of crystallization are not coordinated and each copper(II) ion is four coordinated: Cu(1) is square planar, the sum of the angles around Cu(1) being 360.0(2)° while Cu(2) is tetrahedrally distorted, the total angle amounting to 364.9(2)° and the two planes, [Cu(2), O(1), N(6)] and [Cu(2), N(3), N(4)] making a dihedral angle of 25.4(2)°. The two least squared planes of coordination around the copper ions are not coplanar to each other and make a dihedral angle of 14.6(1)°. The bridging oxygen atom, O(1), is trigonal planar within experimental error (the sum of the angles around O(1) is 359.8(3)°) and hence, in an $sp^2$ hybridization.

The bond distances and angles are in the usual range [5] but the two halves, Cu(1) and Cu(2) coordination spheres, are not equivalent because the two halves of the pmm ligand is intrinsically different. The angle N(2)–Cu(1)–O(1) (included in a five-membered chelate ring) is 82.6(2)° but N(3)–Cu(2)–O(1) (comprised in a six-membered one) is 93.6(2)°. Some differences in coordination bond lengths are noticeable between the two halves. The mutually trans bonds, Cu(1)—O(1) and Cu(1)—N(1) of the Cu(1) moiety are longer than the corresponding Cu(2)—O(1) and Cu(2)—N(4) of the Cu(2) moiety, while the pair, Cu(1)—N(2) and Cu(1)—N(5) of the former are shorter than Cu(2)—N(3) and Cu(2)—N(6) of the latter, respectively. The relative bond distances bridging the alkoxo–O atom, Cu(1)—O(1) {[1.914(3) Å], composing a five-membered chelate ring} and Cu(2)—O(1) {[1.887(3) Å], composing a six-membered one} are in the inverse trend compared with that reported for the two related $\mu$-pyrazolato bridged, Schiff base complexes, the ligands being derived from 1,3-diamino-2-propanol and 1,5-diamino-3-pentanol with salicylaldehyde [5]. That is, the Cu—O (bridged alkoxo oxygen) bond in question is short (1.918 Å) if

Table 1. Colours and analytical results of the new compounds[a]

| Compound ; Colour | Analysis, Found (Calcd.) | | | | |
|---|---|---|---|---|---|
| | C % | H % | N % | M %[b] | $H_2O$ % |
| $Cu_2(OH)(lpm)\cdot 3.5H_2O$ | 36.8 | 4.3 | 10.7 | 24.3 | 12.1 |
| dark blue | (37.1) | (4.5) | (10.8) | (24.5) | (12.2) |
| $Cu_2(pz)(lpm)\cdot 3H_2O$ | 40.9 | 4.2 | 15.2 | 22.5 | 9.6 |
| purple | (40.8) | (4.3) | (15.0) | (22.7) | (9.7) |
| $Cu_2(OAc)(lpm)\cdot 3H_2O$ | 39.1 | 4.3 | 10.1 | 23.0 | 9.7 |
| violet–blue | (39.2) | (4.4) | (10.2) | (23.0) | (9.8) |
| $Cu_2(NO_2)(lpm)\cdot 4.5H_2O$ | 33.7 | 4.2 | 12.2 | 22.4 | 14.6 |
| violet–blue | (34.0) | (4.3) | (12.4) | (22.5) | (14.3) |
| $CuNi(pz)(lpm)\cdot 2H_2O$ | 42.6 | 4.0 | 15.6 | 22.8[c] | 6.7 |
| purple–brown | (42.5) | (4.1) | (15.7) | (22.8) | (6.7) |
| $Ni_2(pz)(lpm)\cdot 2H_2O$ | 42.9 | 4.1 | 15.8 | 22.2 | 6.5 |
| brown | (42.9) | (4.2) | (15.8) | (22.1) | (6.8) |
| $Cu_2Cl(pmm)\cdot 4H_2O$ | 35.1 | 4.2 | 10.3 | 23.3 | 13.6 |
| blue | (35.2) | (4.3) | (10.3) | (23.3) | (13.2) |
| $Cu_2(OH)(pmm)\cdot 3.5H_2O$ | 36.9 | 4.1 | 10.7 | 24.5 | 12.3 |
| dark blue | (37.1) | (4.5) | (10.8) | (24.5) | (12.2) |
| $Cu_2(pz)(pmm)\cdot 3H_2O$ | 40.6 | 4.3 | 14.9 | 22.8 | 9.9 |
| reddish violet | (40.8) | (4.3) | (15.0) | (22.7) | (9.7) |
| $Cu_2(OAc)(pmm)\cdot 4H_2O$ | 38.2 | 4.3 | 9.9 | 22.3 | 12.3 |
| dark blue | (38.0) | (4.6) | (9.8) | (22.3) | (12.7) |
| $Cu_2(NO_2)(pmm)\cdot 5H_2O$ | 33.7 | 4.1 | 12.2 | 22.2 | 15.5 |
| dark blue | (33.5) | (4.4) | (12.2) | (22.1) | (15.7) |
| $CuNi(pz)(pmm)\cdot 5H_2O$ | 38.4 | 4.3 | 14.2 | 20.5[c] | 15.7 |
| brown–violet | (38.6) | (4.8) | (14.2) | (20.7) | (15.2) |
| $Ni_2(pz)(pmm)\cdot 5H_2O$ | 38.9 | 4.3 | 14.3 | 20.0 | 15.7 |
| brown | (39.0) | (4.8) | (14.3) | (20.0) | (15.4) |
| $Cu_2(OH)(lpe)\cdot 4H_2O$ | 38.9 | 4.8 | 10.1 | 22.9 | 13.1 |
| green–blue | (39.0) | (5.1) | (10.1) | (22.9) | (13.0) |
| $Cu_2(pz)(lpe)\cdot H_2O$ | 46.1 | 4.3 | 15.1 | 23.1 | 3.1 |
| brownish purple | (45.7) | (4.4) | (15.2) | (23.0) | (3.3) |
| $Cu_2(OH)(pem)\cdot 4.5H_2O$ | 38.4 | 4.8 | 10.0 | 22.6 | 14.0 |
| green–blue | (38.3) | (5.2) | (9.9) | (22.5) | (14.4) |
| $Cu_2(pz)(pem)\cdot 0.5H_2O$ | 46.7 | 4.3 | 15.2 | 23.4 | 1.7 |
| brownish purple | (46.5) | (4.3) | (15.5) | (23.4) | (1.7) |
| $Cu_2Cl(pmg)\cdot 4H_2O$[d] | 36.6 | 4.4 | 10.1 | 22.7 | 12.7 |
| sky blue | (36.5) | (4.5) | (10.0) | (22.7) | (12.9) |
| $Cu_2(OH)(pmg)\cdot 4.5H_2O$ | 37.0 | 4.6 | 10.2 | 23.3 | 14.7 |
| dark blue | (37.1) | (4.9) | (10.2) | (23.1) | (14.7) |
| $Cu_2(pz)(pmg)\cdot 2H_2O$ | 42.9 | 4.4 | 14.7 | 22.9 | 6.8 |
| reddish violet | (43.2) | (4.4) | (15.1) | (22.9) | (6.5) |
| $Cu_2(OAc)(pmg)\cdot 8H_2O$ | 35.0 | 5.3 | 8.6 | 19.2 | 21.8 |
| blue | (34.8) | (5.5) | (8.6) | (19.4) | (22.0) |

[a] Abbreviations: pz = pyrazolate ion, OAc = acetate ion, lpm = N,N′-bis(2-pyridylmethyl)-(S)-malamide anion, pmm = N,N′-bis(2-pyridylmethyl)-(R,S)-malamide anion, lpe = N,N′-bis{2-(2-pyridyl)ethyl}-(S)-malamide anion, pem = N,N′-bis{2-(2-pyridyl)-ethyl}-(R,S)-malamide anion, and pmg = N,N′-bis(2-pyridyl-methyl)-3-hydroxyglutaramide anion.

[b] M = Cu or Ni.

[c] M = Cu + Ni.

[d] Cl analysis: Found 6.2%, Calcd. 6.3%.

it is a member of the five-membered chelate rings formed with the former Schiff base and long (1.942 and 1.961 Å) if it is a member of the six-membered ones with the latter. The origin is not clear so far but cumulative chelate rings should have an influence on the varying bond lengths. The relatively short Cu(1)—O(1) and Cu(2)—O(1) bonds and nearly perfect planarity of the O(1) atom should be reflected in the magnetic property of the amide complex, $Cu_2(pz)(pmm)\cdot 3H_2O$.

The chirality of asymmetric C(8) of one enantiomer shown in Fig. 4 is S and the chirality of the tetrahedrally distorted Cu(2) is Δ. In the crystals the center of symmetry lies on the middle point between the

Table 2. Intramolecular bond distances (Å) and angles (°) of $Cu_2(pz)(pmm)\cdot 3H_2O$ with e.s.d. in parentheses

| | | | |
|---|---|---|---|
| Cu(1)—Cu(2) | 3.3727(9) | N(4)—C(16) | 1.347(7) |
| Cu(1)—O(1) | 1.914(3) | N(5)—N(6) | 1.369(6) |
| Cu(1)—N(1) | 2.049(4) | N(5)—C(17) | 1.348(7) |
| Cu(1)—N(2) | 1.879(4) | N(6)—C(19) | 1.326(7) |
| Cu(1)—N(5) | 1.952(4) | C(1)—C(2) | 1.367(8) |
| Cu(2)—O(1) | 1.887(3) | C(2)—C(3) | 1.36(1) |
| Cu(2)—N(3) | 1.928(4) | C(3)—C(4) | 1.383(9) |
| Cu(2)—N(4) | 1.999(4) | C(4)—C(5) | 1.396(8) |
| Cu(2)—N(6) | 1.979(4) | C(5)—C(6) | 1.497(7) |
| O(1)—C(8) | 1.412(6) | C(7)—C(8) | 1.527(7) |
| O(2)—C(7) | 1.259(7) | C(8)—C(9) | 1.507(8) |
| O(3)—C(10) | 1.245(6) | C(9)—C(10) | 1.518(7) |
| N(1)—C(1) | 1.362(7) | C(11)—C(12) | 1.496(7) |
| N(1)—C(5) | 1.331(8) | C(12)—C(13) | 1.377(7) |
| N(2)—C(6) | 1.462(7) | C(13)—C(14) | 1.371(8) |
| N(2)—C(7) | 1.310(6) | C(14)—C(15) | 1.392(9) |
| N(3)—C(10) | 1.315(6) | C(15)—C(16) | 1.363(8) |
| N(3)—C(11) | 1.467(6) | C(17)—C(18) | 1.343(9) |
| N(4)—C(12) | 1.346(6) | C(18)—C(19) | 1.385(8) |

| | | | |
|---|---|---|---|
| O(1)—Cu(1)—N(1) | 164.3(2) | Cu(2)—N(6)—C(19) | 129.9(4) |
| O(1)—Cu(1)—N(2) | 82.6(2) | N(5)—N(6)—C(19) | 107.8(4) |
| O(1)—Cu(1)—N(5) | 87.4(2) | N(1)—C(1)—C(2) | 121.9(6) |
| N(1)—Cu(1)—N(2) | 81.8(2) | C(1)—C(2)—C(3) | 119.7(6) |
| N(1)—Cu(1)—N(5) | 108.2(2) | C(2)—C(3)—C(4) | 119.4(6) |
| N(2)—Cu(1)—N(5) | 170.0(2) | C(3)—C(4)—C(5) | 118.7(6) |
| O(1)—Cu(2)—N(3) | 93.6(2) | N(1)—C(5)—C(4) | 121.7(5) |
| O(1)—Cu(2)—N(4) | 164.2(2) | N(1)—C(5)—C(6) | 118.1(4) |
| O(1)—Cu(2)—N(6) | 86.0(2) | C(4)—C(5)—C(6) | 120.2(5) |
| N(3)—Cu(2)—N(4) | 83.9(2) | N(2)—C(6)—C(5) | 107.4(4) |
| N(3)—Cu(2)—N(6) | 160.8(2) | O(2)—C(7)—N(2) | 127.1(5) |
| N(4)—Cu(2)—N(6) | 101.4(2) | O(2)—C(7)—C(8) | 120.8(4) |
| Cu(1)—O(1)—Cu(2) | 125.1(2) | N(2)—C(7)—C(8) | 112.1(5) |
| Cu(1)—O(1)—C(8) | 115.6(3) | O(1)—C(8)—C(7) | 109.9(4) |
| Cu(2)—O(1)—C(8) | 119.1(3) | O(1)—C(8)—C(9) | 111.3(4) |
| Cu(1)—N(1)—C(1) | 128.4(4) | C(7)—C(8)—C(9) | 111.3(4) |
| Cu(1)—N(1)—C(5) | 112.6(3) | C(8)—C(9)—C(10) | 116.4(4) |
| C(1)—N(1)—C(5) | 118.6(4) | O(3)—C(10)—N(3) | 123.6(5) |
| Cu(1)—N(2)—C(6) | 119.5(3) | O(3)—C(10)—C(9) | 119.1(4) |
| Cu(1)—N(2)—C(7) | 119.8(4) | N(3)—C(10)—C(9) | 117.4(4) |
| C(6)—N(2)—C(7) | 120.7(4) | N(3)—C(11)—C(12) | 110.4(4) |
| Cu(2)—N(3)—C(10) | 129.7(3) | N(4)—C(12)—C(11) | 116.9(4) |
| Cu(2)—N(3)—C(11) | 113.6(3) | N(4)—C(12)—C(13) | 121.5(5) |
| C(10)—N(3)—C(11) | 115.2(4) | C(11)—C(12)—C(13) | 121.6(4) |
| Cu(2)—N(4)—C(12) | 113.0(3) | C(12)—C(13)—C(14) | 120.1(5) |
| Cu(2)—N(4)—C(16) | 129.6(3) | C(13)—C(14)—C(15) | 119.0(5) |
| C(12)—N(4)—C(16) | 117.4(4) | C(14)—C(15)—C(16) | 117.5(5) |
| Cu(1)—N(5)—N(6) | 119.3(3) | N(4)—C(16)—C(15) | 124.3(5) |
| Cu(1)—N(5)—C(17) | 134.8(4) | N(5)—C(17)—C(18) | 112.1(5) |
| N(6)—N(5)—C(17) | 105.9(4) | C(17)—C(18)—C(19) | 103.5(5) |
| Cu(2)—N(6)—N(5) | 121.8(3) | N(6)—C(19)—C(18) | 110.7(5) |

two Cu(1) atoms and the distance between Cu(1) and Cu(1′) is 3.627(1). The closest atom to Cu(1) is N(1′) with a separation of 3.400(4) Å. The asymmetric arrangement of the two terminal pyridine rings relative to each other is also controlled to Δ and the dihedral angle is 34.1(2)°. These chiralities are reflected on CD spectra of optically active $Cu_2(pz)(lpm)\cdot 3H_2O$ discussed below.

On complexation with copper(II) ions, the amide I and II bands of free ligands received a characteristic change: strong bands were observed between 1619–1542 $cm^{-1}$ suggesting that the deprotonated amide–

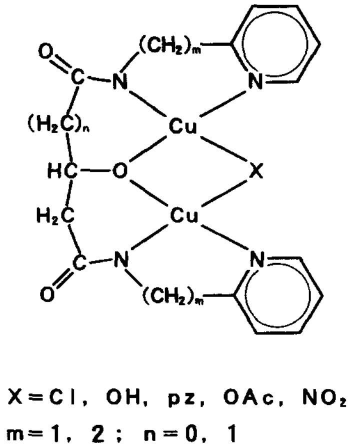

Fig. 3. Binuclear copper(II) complexes. OAc is an acetate ion and pz is a pyrazolate ion.

N atoms are coordinated [6] (Fig. 3). The presence of water of crystallization makes the 3000–3500 $cm^{-1}$ region not informative: the absence of $\nu$(NH) of the amide groups and of $\nu$(OH) of the alcohol group is not directly confirmed but the analytical results reveal the trivalent anionic nature of the ligands: the alcohol and two amide groups are deprotonated.

The acetato complexes, $Cu_2(OAc)(L) \cdot nH_2O$ (L = lpm, pmm, pmg), have two unique strong bands which are not observed for the IR spectra of the other complexes: 1545 and 1448 (lpm), 1549 and 1455 (pmm), 1556 and 1445 $cm^{-1}$ (pmg), the positions of which indicate that the OAc group is symmetrically coordinated through the two O atoms [7]. In the IR spectra of the nitrito complexes, $Cu_2(NO_2)(L) \cdot nH_2O$ (L = lpm, pmm), two characteristic peaks at 1456 and 1212 $cm^{-1}$ are assigned to the bands due to an $NO_2$ group and the frequencies are close to those observed for $NO_2$ coordinating through N and O atoms (i.e. an M—N(=O)—O—M arrangement) [7]. This coordination mode of $NO_2$ has been confirmed by X-ray analysis for (1,2-$\mu$-nitrito)(N,N,N′,N′-tetrakis[2-(1-ethylbenzimidazolyl)methyl]-2-hydroxy-1,3-diaminopropanato)-dicopper(II) diperchlorate [8]. In the coordination mode two isomers are possible because the two Cu(II) centers are not equivalent (Fig. 3, $n = 0$, $m = 1$), but the problem can not be solved without X-ray structural analysis.

The magnetic moments at room temperature (Table 3) depend markedly upon both L and X. The two complexes, $Cu_2X(pmg) \cdot nH_2O$ (X = OAc and Cl), are magnetically normal and the moments of $Cu_2(OH)(L) \cdot nH_2O$ (L = pmg, pem, lpe) are slightly subnormal. The pz complexes are all quite subnormal indicating the presence of strong antiferromagnetic interaction between two Cu atoms. The interaction decreases in the order of X, pz > $NO_2$ > OH > Cl, OAc and is weak for the pmg complexes. To obtain reliable information, the temperature dependence of the magnetic susceptibilities of the optically active 'lpm' complexes were measured. The susceptibilities are approximated by Bleaney–Bowers expression assuming a dimer (Fig. 3). The result is given in Table 4 (J is based on the formula, $H = -2JS_1 \cdot S_2$) and the antiferromagnetic interaction decreases in the above order of X. Magnetic interaction between two copper(II) atoms of this type of dimer has been shown to be very susceptible to the fine structure and also shown that the *exo* bridging X pathway can be either complementary or counter-complementary to the *endo*

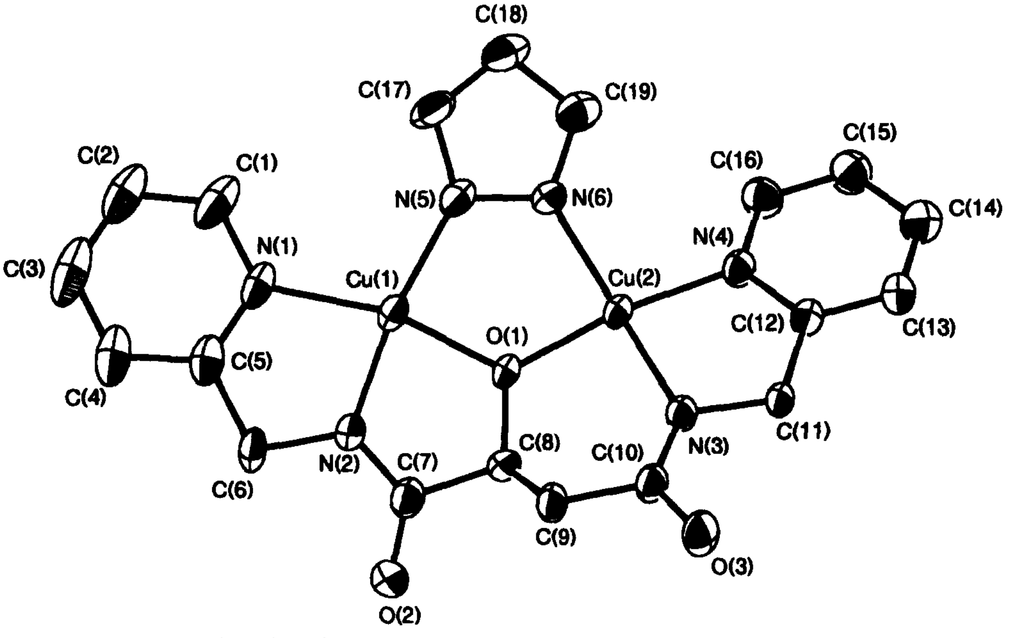

Fig. 4. ORTEP view of $Cu_2(pz)(pmm) \cdot 3H_2O$ together with atom numbering scheme.

Table 3. Magnetic moments ($\mu_{eff}$, B.M.)[a] at room temperature, electronic spectra ( × $10^3$ $cm^{-1}$)[b] and amide bands in infrared spectra ($cm^{-1}$) of Nujol mulls of the complexes

| Complex | $\mu_{eff}$ | Electronic spectra | Amide band |
|---|---|---|---|
| $Cu_2(OH)(lpm) \cdot 3.5H_2O$ | 0.78 | 16.7, 28.9 | 1606, 1565 |
| $Cu_2(pz)(lpm) \cdot 3H_2O$ | 0.67 | 17.4, 27.3 | 1609, 1558 |
| $Cu_2(OAc)(lpm) \cdot 3H_2O$ | 1.43 | 17.0, 28.1 | 1619, 1563 |
| $Cu_2(NO_2)(lpm) \cdot 4.5H_2O$ | 0.77 | 17.3, 27.7 | 1593, 1545 |
| $CuNi(pz)(lpm) \cdot 2H_2O$ | 1.25[c] | 18.3sh, 22.2, 31.6 | 1622, 1615 |
| $Ni_2(pz)(lpm) \cdot 2H_2O$ | dia | 17.9sh, 22.0, 31.6 | 1624, 1609 |
| $Cu_2Cl(pmm) \cdot 4H_2O$ | 0.98 | 15.8, 30.2 | 1602, 1543 |
| $Cu_2(OH)(pmm) \cdot 3.5H_2O$ | 0.83 | 16.9, 29.4 | 1604, 1561 |
| $Cu_2(pz)(pmm) \cdot 3H_2O$ | 0.54 | 17.7, 27.9 | 1592, 1562 |
| $Cu_2(OAc)(pmm) \cdot 4H_2O$ | 1.28 | 16.9, 28.3 | 1608, 1562 |
| $Cu_2(NO_2)(pmm) \cdot 5H_2O$ | 0.78 | 17.3, 27.8 | 1593, 1547 |
| $CuNi(pz)(pmm) \cdot 5H_2O$ | 1.53[c] | 18.5sh, 22.3, 32.6 | 1626, 1610 |
| $Ni_2(pz)(pmm) \cdot 5H_2O$ | dia | 17.9sh, 22.1, 32.3 | 1627, 1611 |
| $Cu_2(OH)(lpe) \cdot 4H_2O$ | 1.71 | 16.0, 26.1sh | 1577, 1542 |
| $Cu_2(pz)(lpe) \cdot H_2O$ | 0.64 | 18.6, 26.1 | 1594, 1544 |
| $Cu_2(OH)(pem) \cdot 4.5H_2O$ | 1.68 | 16.0, 25.8sh | 1577, 1542 |
| $Cu_2(pz)(pem) \cdot 0.5H_2O$ | 0.61 | 18.7, 26.4 | 1594, 1545 |
| $Cu_2Cl(pmg) \cdot 4H_2O$ | 1.99 | 16.0, 31.7sh[d] | 1578, 1549 |
| $Cu_2(OH)(pmg) \cdot 4.5H_2O$ | 1.63 | 17.1, 27.0 | 1577, 1543 |
| $Cu_2(pz)(pmg) \cdot 2H_2O$ | 0.78 | 18.0, 19.3sh, 28.2 | 1579, 1566 |
| $Cu_2(OAc)(pmg) \cdot 8H_2O$ | 1.83 | 15.6, 27.8sh[d] | 1580, 1556 |

[a] $\mu_{eff}$ is represented per metal ion. dia = diamagnetic.

[b] sh = shoulder.

[c] $\mu_{eff}$ was calculated on the assumption that Ni was diamagnetic.

[d] The shoulder is a very slight swell on a lower energy side of strong high energy bands and the position is uncertain.

Table 4. Magnetic parameters for $Cu_2X(lpm) \cdot nH_2O$ (X = OH, pz, OAc, and $NO_2$)

| Complex | $J/cm^{-1}$ | $g$ |
|---|---|---|
| $Cu_2(OH)(lpm) \cdot 3.5H_2O$ | −385 | 2.22 |
| $Cu_2(pz)(lpm) \cdot 3H_2O$ | −452 | 2.25 |
| $Cu_2(OAc)(lpm) \cdot 3H_2O$ | −155 | 2.19 |
| $Cu_2(NO_2)(lpm) \cdot 4.5H_2O$ | −446 | 2.45 |

alkoxo–O pathway in the interaction [5,9]. This is the case for the present complexes.

It seems reasonable to assume that the Cu–O–Cu angle of the *endo*-bridge decreases when a triatomic O–C–O *exo*-bridge of OAc is replaced with a diatomic NN *exo*-bridge of pz and the antiferromagnetic interaction would be reduced : the antiferromagnetic interaction through a Cu–O–Cu pathway is experimentally established to decrease with a decreasing Cu–O–Cu angle (when the angle > 97.5°) [10]. The replacement of OAc with pz in the present complexes, however, strengthens the antiferromagnetic interaction (Table 4). This fact is qualitatively explained in the view of O. Kahn [10] : in $Cu_2(OAc)(lpm) \cdot 3H_2O$ the carboxylato part exerts a countercomplementarity effect and the magnitude of antiferromagnetic interaction is small but in $Cu_2(pz)(lpm) \cdot 3H_2O$ the pz bridge exerts complementarity effect and the magnitude is large. The observed effect of the replacement is not so drastic as the reported case when OAc was replaced with $N_3$, both OAc and $N_3$ *exo*-bridges being triatomic and the endo Cu–O–Cu angle being not reduced by the replacement [10].

In the solid electronic spectra of the two magnetically normal complexes (Table 3) the band in the near UV region is very faint but the band is distinctly observed for magnetically subnormal complexes. This type of band has been interpreted as an LMCT transition from the bridged alkoxy–O (having a trigonal planar geometry) to Cu atoms [11]. The LMCT transition seems to be practically forbidden for the two magnetically normal complexes probably because distortion from a trigonal planar toward a pyramidal geometry of the endogenous bridging alkoxy–O atom is induced by unfavorable size of fused chelate rings and *exo*-bridging groups, that is, the two copper coordination spheres are folded relative to each other. This results also in disruption of magnetic interaction.

The magnetic moments of the $NO_2$ complexes are rather close to those of the pz ones but significantly different from those of the OAc complexes (Tables 3 and 4). In the pz complexes, the additional magnetic interaction due to the *exo*-bridge occurs through a Cu—N—N—Cu arrangement while in the OAc one through a Cu—O—C—O—Cu path. The similarity in magnetic moments of the $NO_2$ complexes to the pz one should, in first approximation, suggest that the interaction occurs through a Cu—N(=O)—O—Cu arrangement rather than through Cu—O—N—O—Cu arrangement. This assumption is consistent with the IR result mentioned above.

The absorption maxima of solid $Cu_2X(L)\cdot nH_2O$ in the ligand field transition region shift as expected from ligand field strength [12] of X when L is the same (except $H_3pmg$), but the L-dependent shifts are not so clear. Ring sizes of fused chelating ligands are known to be an important factor determining a ligand field strength around $Cu^{II}$ [12], but the complexes studied in this work being dimeric and the two halves being not equivalent [except $H_3(pmg)$], there is no simple situation. Apical coordination, which also affects the transition energies as well, should complicate the phenomena. Marked colour changes upon dehydration of some complexes indicate interaction of water of crystallization with a copper(II) ion in axial coordination sites.

The absorption spectra of some of the complexes in ethanol or methanol are measured (Table 5) and the spectra are essentially similar to those of the solid samples; in the visible region *d–d* transitions are observed and more strong LMCT bands in the near UV region. The latter bands are very indistinct also for the magnetically normal copper(II) complexes as in the solid state. The molar extinction coefficients

Table 5. Absorption (AB) and circular dichroism (CD) spectra of some of the complexes[a]

| Complex | AB/CD spectra, in $10^3$ $cm^{-1}$ (log ε/Δε) | | |
|---|---|---|---|
| $Cu_2(OH)(lpm)\cdot 3.5H_2O$ | AB16.2 (2.48), | 30.0 (3.50), | 37.6 (4.08) |
| | CD14.2 (+0.47), | 25.0 (+0.18), | 37.0 (−9.41) |
| | 16.9 (−0.69), | 27.6 (−0.22) | |
| | 19.8 (+0.08) | 30.7 (+0.39) | |
| $Cu_2(pz)(lpm)\cdot 3H_2O$ | AB17.5 (2.77) | 28.2 (3.59), | 37.6 (4.07) |
| | CD15.0sh (+0.3), | 27.9 (−2.32), | 37.0 (−10.05) |
| | 18.2 (+1.20) | 33.0 (+0.38) | |
| | 22.0sh (−0.1) | | |
| $Cu_2(OAc)(lpm)\cdot 3H_2O$ | AB16.3 (2.53), | 29.4 (3.32), | 37.8 (4.10) |
| | CD14.7 (−0.45), | 24.4 (−0.01), | 37.6 (−17.69) |
| | 17.4 (+1.00), | 31.3 (+1.00) | |
| $Cu_2(NO_2)(lpm)\cdot 4.5H_2O$ | AB17.2 (2.74), | 27.8 (3.47), | 37.7 (4.12) |
| | | 33.4sh (3.6) | |
| | CD14.0 (+0.10), | 26.5 (−0.86), | 37.3 (−12.95) |
| | 15.7 (−0.10), | 31.5 (+1.02) | |
| | 18.2 (+1.17) | | |
| $CuNi(pz)(lpm)\cdot 2H_2O$ | AB18.1 (2.32), | 31.5 (3.77), | 37.6sh (3.9) |
| | 22.5 (2.53), | | 42.6 (4.32) |
| | CD16.6 (+0.65), | 31.2 (−1.81), | 37.3sh (−5.5) |
| | 21.4 (−0.55), | | 40.7 (−15.80) |
| $Ni_2(pz)(lpm)\cdot 2H_2O$ | AB18.6sh (2.1), | 31.6 (3.92), | 42.9 (4.38) |
| | 22.4 (2.66) | | |
| | CD17.9 (+0.90), | 29.2 (−0.79), | 40.8 (−19.77) |
| | 22.2 (−1.43), | 33.3 (−1.76) | |
| $Cu_2Cl(pmm)\cdot 4H_2O$ | AB15.8 (2.48), | 30.6 (3.41), | 38.0 (4.09) |
| $Cu_2(OH)(lpe)\cdot 4H_2O$[b] | AB17.1 (2.22), | 26.4 (3.10), | 38.1 (4.16) |
| | | 34.5sh (2.7) | |
| | CD13.2 (−0.03), | 25.0 (−1.17), | 39.6 (−2.36) |
| | 17.0sh (+0.3), | 30.0 (−0.48) | |
| | 19.3 (+0.51), | 34.4 (+2.90) | |
| $Cu_2(pz)(lpe)\cdot H_2O$ | AB18.5 (2.67), | 27.2 (3.70), | 38.0 (4.08) |
| | | 31.0sh (3.4) | |
| | CD15.8 (−0.35), | 26.9 (−3.13), | 38.8 (−5.57) |
| | 18.6 (+1.34), | 32.6 (+3.18) | |
| | 21.7 (−0.59) | | |
| $Cu_2Cl(pmg)\cdot 4H_2O$ | AB16.1 (2.23), | 26.0sh (2.5), | 38.2 (4.14) |
| | | 32.5sh (3.5) | |
| $Cu_2(OH)(pmg)\cdot 4.5H_2O$ | AB17.5 (2.17), | 26.8 (2.70), | 37.6 (4.19) |
| $Cu_2(pz)(pmg)\cdot 2H_2O$ | AB17.4 (2.50), | 27.6 (3.49), | 37.4 (4.08) |
| | | 31.5sh (3.4) | |
| $Cu_2(OAc)(pmg)\cdot 8H_2O$ | AB16.3 (2.27), | 29.0sh (3.0), | 37.7 (4.13) |

[a] Ethanol was used as a solvent unless otherwise noted.

[b] Methanol was used as a solvent because of the low solubility of the complex in ethanol.

(log $\varepsilon$) of the *d–d* bands of the lpm complexes are larger than those of the corresponding pmg complexes and this consists with the experience rule that the $\varepsilon$ values of copper complexes with fused 5-5 membered chelate rings are larger than those of similar complexes with fused 5-6 membered chelate rings [13]: the pmg ligand forms two 5-6 fused chelate rings and lpm a 5-5 and a 5-6 fused chelate ring (Fig. 3). The log $\varepsilon$ values of the lpe complexes are intermediate (lpe forms a 6-5 and a 6-6 fused chelate ring).

The CD (circular dichroism) spectra of the optically active complexes are given in Table 5, which show better resolved components of the electronic transitions than the absorption spectra (typical examples are illustrated in Fig. 5). In the visible region (corresponding to the *d–d* transition region) are observed three components [only two are observed for $Cu_2(OAc)(lpm)\cdot 3H_2O$ but an unsymmetrical tailing of the maximum at $17.4\times 10^3$ cm$^{-1}$ toward higher energy may be indicative of the presence of the 3rd component] and the appearance of three transitions may suggest a tetragonal (or square planar) $d^9$ effective ligand field. The transition $^2B_1g \rightarrow {}^2A_1g$ is, however, magnetic-dipole forbidden and should be very weak or not observable. Lowering the symmetry splits the degenerate $^2Eg$ state into two components and three allowed transitions are expected. Assignments of each component to specific transitions are difficult at present. The rather strong CD spectra should result from a tetrahedrally distorted coordination geometry from a square planar one as indicated by the X-ray structure of $Cu_2(pz)(pmm)\cdot 3H_2O$.

It is noteworthy that in the near UV region two or three components are observed. The absorption in this region has been interpreted to be an LMCT transition from the non-bonding $\pi$ orbital on a bridging alkoxo–O (sp$^2$) atom to an empty *d*-orbital of a Cu ion. The presence of more than one CD component suggests either the splitting of the LMCT transition due to the inequivalence of the two Cu atoms (Fig. 3) or the appearance of an LMCT transition from X to Cu, the dependence of the CD components on the *exo*-bridging X group being indicative of the contribution of the latter LMCT to the CD spectra. Further studies of CD spectra in the near UV region of alkoxo–O bridged, optically active, magnetically subnormal copper(II) complexes will be required for a complete understanding of the results. In the UV region all the copper complexes show a strong negative CD component (Table 5 and Fig. 5) while the free ligand sulfate, $H_3(lpm)\cdot 1\frac{2}{3}H_2SO_4\cdot \frac{1}{3}CH_3OH$, a weak CD spectrum: $\nu_{ext} = 38.31\times 10^3$ cm$^{-1}$ ($\Delta\varepsilon = +0.67$) [absorption spectrum ($CH_3OH$): $\nu_{max} = 38.21$, log $\varepsilon = 4.02$]. The enhanced CD spectra of the complexes are interpreted as the result of the fixed framework of the coordinated ligand: for instance, the two terminal pyridine rings are fixed in a chiral arrangement relative to each other restricted by the asymmetric carbon (cf. C(8) of Fig. 4).

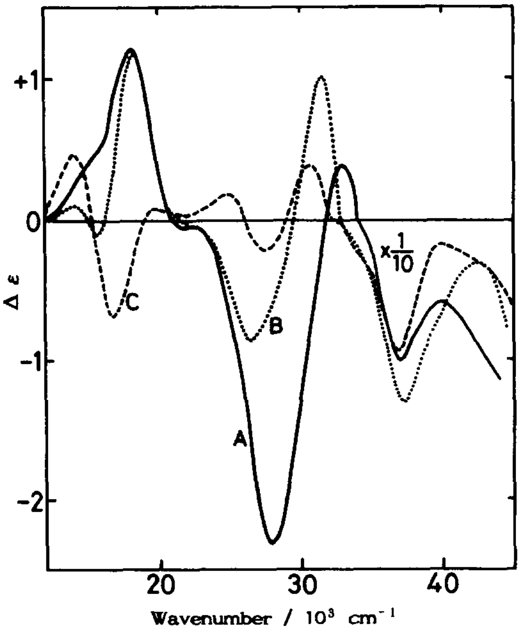

Fig. 5. CD spectra of ethanol solutions of $Cu_2(pz)(lpm)\cdot 3H_2O$ (A), $Cu_2(NO_2)(lpm)\cdot 4.5H_2O$ (B), and $Cu_2(OH)(lpm)\cdot 3.5H_2O$ (C).

The square planar nickel complex shows two CD components in the *d–d* transition region corresponding to the absorption spectrum (Table 5). Two transitions are expected for a low spin $d^8$, $D_{4h}$ symmetry ligand field because the transition $^1A_1g \rightarrow {}^1B_2g$ are magnetic-dipole forbidden. The CD spectra in the near UV and UV region originated from LMCT and intraligand transitions resemble those of the above discussed copper complexes.

In the heterometallic complex, $CuNi(pz)(lpm)\cdot 2H_2O$, the characteristic band at $28.2\times 10^3$ cm$^{-1}$ of the LMCT from the bridging oxygen to the copper ions of $Cu_2(pz)(lpm)\cdot 3H_2O$ disappeared (Table 5), but in the *d–d* transition region, the spectral pattern is similar to the sum of the absorptions due to $Cu_2(pz)(lpm)\cdot 3H_2O$ and $Ni_2(pz)(lpm)\cdot 2H_2O$. On the other hand the CD spectrum of $CuNi(pz)(lpm)\cdot 2H_2O$ is not the arithmatic mean of those of the two homometallic complexes: the difference is quite plain in the LMCT region. $CuNi(pz)(lpm)\cdot 2H_2O$ is, therefore, not a mere mixture of the two homometallic complexes. These facts suggest that the dimeric $Cu_2$ unit is broken off and that the Ni part is square planar in the heterometallic complex. If the Ni part is diamagnetic and there is no intermolecular magnetic interaction, the Cu ion would be magnetically normal. The observed moment is subnormal and the assumption is not correct. The temperature dependence of the magnetic susceptibility is depicted in Fig. 6. The best fit curve to measured points was obtained by assuming that the complex was, magnetically, a mixture of a 1/4 mole of $Ni_2(pz)(lpm)$, a 1/2 mole of $CuNi(pz)(lpm)$, and a 1/4 mole of $Cu_2(pz)(lpm)$: $Ni_2(pz)(lpm)$ was diamagnetic, $CuNi(pz)(lpm)$ was

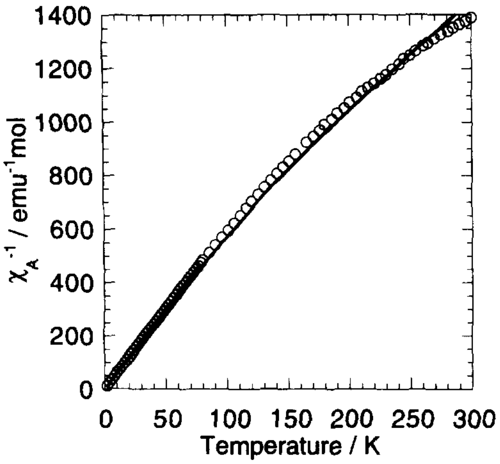

Fig. 6. Temperature dependence of magnetic susceptibility of CuNi(pz)(lpm) · $2H_2O$. The solid line is calculated on the assumption given in the text.

composed of a diamagnetic Ni and a magnetically normal Cu atom, and $Cu_2$(pz)(lpm) had the identical magnetic property to that of pure $Cu_2$(pz)(lpm) discussed above. There remains another problem in that the two coordination sites of lpm (and pmm) are not equivalent and two isomers are possible for the heterometallic complexes. So far no crystals suitable for X-ray analysis are not obtained but we propose that the $Ni^{II}$ ion (smaller size) prefers the coordination site surrounded by a fused 5-5 membered chelate ring and the Cu(II) ion the one surrounded by a 5-6 part[13].

## EXPERIMENTAL

### *Measurements*

Infrared spectra were measured on a Perkin–Elmer System 2000 FTIR spectrophotometer as Nujol mulls and if necessary as hexachlorobutadiene mulls (in the region, 1500–1300 $cm^{-1}$). NMR spectra were recorded on a Hitachi R-90H spectrometer and referenced to internal tetramethylsilane. Visible and UV spectra were obtained on a Hitachi U-3400 spectrophotometer.

Absorption spectra were measured of *ca* $10^{-3}$ mole/$dm^3$ solutions and solid spectra were obtained by Nujol mull method. Magnetic moments at room temperature were determined by the Gouy method and water was used as a standard. Temperature dependent magnetic susceptibilities were measured by the Faraday method between 4 K and room temperature as reported previously [14].

### *Synthesis of the ligands*

$H_3$(pmg). A mixture of 0.1 mol (20.4 g) of diethyl-3-hydroxy-glutarate and 0.2 mole (21.6 g) of 2-aminomethylpyridine was heated in an oil bath (130°C) for 3 h and allowed to cool to room temperature. The resulted white solid was recrystallized from hot ethanol to give the product in 40% yield. M.p. 137–138°C. Found: C, 62.26; H, 6.11; N, 17.13%. Calcd: C, 62.18; H, 6.14; N, 17.06%. IR, 1650 (amide I), 1567 and 1538 $cm^{-1}$ (amide II). NMR (dimethylsulfoxide-$d_6$ [dmso-$d_6$]), $^1H$: $\delta = 2.41$ ppm (d, $J = 6.4$ Hz, $CH_2$), 4.33 (m, CH), 4.42 (d, 5.9, $CH_2$), 5.08 (d, 5.1, OH), 7.31 (m, pyridyl (py) H-3,5), 7.77 (td, 7.6, 1.8, H-4), 8.45 (br, t, 5.9, NH), 8.51 (ddd, 4.8, 1.8, 1.0, py H-6); $^{13}C\{^1H\}$: $\delta = 43.3$ ppm, 44.1 ($CH_2$), 63.4 (CH), 120.8, 121.8, 136.5, 148.5, 158.4 (py), 170.5 (C═O).

In a similar manner, $H_3$(pem) and $H_3$(lpe) were obtained from 2-(2-aminoethyl)pyridine (24.4 g) and dimethyl-(R,S)-malate (16.2 g) or dimethyl-(S)-malate (16.2 g), respectively. For recrystallization of $H_3$(pem), the hot ethanol solution was treated with charcoal and the yield was 60%. $H_3$(pem): m.p. 130–131°C. Found: C, 62.86; H, 6.50; N, 16.38%. Calcd: C, 63.14; H, 6.48; N, 16.36%. IR, 1675 and 1636 (amide I), 1562 and 1520 $cm^{-1}$ (amide II). NMR (dmso-$d_6$), $^1H$: 2.44 ppm (m, $CH_2$), 2.92 (m, $CH_2$), 3.43 (m, $CH_2$), 4.30 (m, CH), 5.77 (d, 5.7 Hz, OH), 7.23 (m, py H-3,5), 7.73 (m, py H-4), 7.95 (br, NH), 8.52 (m, py H-6); $^{13}C\{^1H\}$: 37.1 ppm, 37.3, 38.0, 38.5, 40.8 ($CH_2$), 68.5 (CH), 121.3, 122.9, 136.2, 148.8, 158.8, 158.9 (py), 169.8, 172.9 (C═O).

$H_3$(lpe) was not solidified and formed no solid salt with acid. The concentrated oily residue was, therefore, used for preparation of complexes without purification. IR ($CDCl_3$ solution), 1600 (amide I), 1530 $cm^{-1}$ (amide II). NMR ($CDCl_3$), $^1H$: 2.44 ppm (dd, 8.1 Hz, 14.9, $CH_2$), 2.86 (dd, 3.7, 15.2, $CH_2$), 2.97 (m, $CH_2$), 3.62 (m, $CH_2$), 4.37 (dd, 4.0, 8.1, CH), 5.27 (br, OH), 7.12 (m, py H-3,5), 7.42 (br, NH), 7.58 (m, py H-4), 7.63 (br, NH), 8.46 (m, py H-6); $^{13}C$: 36.9 ppm, 37.2, 38.4, 38.8, 39.5 ($CH_2$), 69.1 (CH), 121.3, 121.4, 123.1, 123.2, 136.3, 136.5, 148.8, 149.0, 158.8, 158.9 (py), 171.5, 172.7 (C═O).

$H_3$(pmm) · $1.5H_2SO_4$ · $0.5CH_3OH$ and $H_3$(lpm) · 12/$3H_2SO_4$ · 1/$3CH_3OH$. A mixture of 0.1 mole (16.2 g) of dimethyl-(R,S)-malate or dimethyl-(S)-malate, respectively, and 0.2 mole (21.6 g) of 2-aminomethylpyridine was heated in an oil bath (130°C) for 3 h and allowed to cool to room temperature. The oily residue was treated with 0.2 mole (19.6 g) of sulfuric acid diluted with 100 mL of ethanol to give a solid. The supernatant liquid was discarded and the solid was recrystallized from about 600 mL of methanol to give a hygroscopic white solid in a yield of 60%.

$H_3$(pmm) · $1.5H_2SO_4$ · $0.5CH_3OH$. M.p. 152–155°C. Found: C, 42.02; H, 4.88; N, 11.79%. Calcd: C, 41.51; H, 4.43; N, 11.73%. IR, 1675 (amide I), 1530 $cm^{-1}$ (amide II). NMR (dmso-$d_6$), $^1H$: 2.68 ppm (m, $CH_2$), 3.21 (s, $CH_3OH$), 4.46 (m, CH), 4.65 (d, 5.1 Hz, $CH_2$), 7.79 (m, py H-3,5), 8.37 (m, py H-4), 8.77 (m, py H-6); $^{13}C\{^1H\}$: 41.1 ppm, 42.3 ($CH_2$), 48.6 ($CH_3OH$), 68.4 (CH), 123.8, 123.9, 124.3, 124.4, 143.2, 143.3, 143.4, 143.5, 155.2, 155.4 (py), 170.7, 174.0 (C=O). One of the $^{13}C(CH_2)$ signals was overlapped with the strong peaks of dmso-$d_6$.

$H_3$(lpm)·12/3$H_2SO_4$·1/3$CH_3OH$. M.p. 166–167°C. Found: C, 39.86; H, 4.51; N, 11.36%. Calcd: C, 40.16; H, 4.68; N, 11.47%. IR, 1672 (amide I), 1532 cm$^{-1}$ (amide II). NMR (dmso-$d_6$), $^1H$: 2.68 ppm (m, $CH_2$), 3.21 (s, $CH_3OH$), 4.45 (m, CH), 4.67 (d, 5.5 Hz, $CH_2$), 7.87 (m, py H-3,5), 8.47 (m, py H-4), 8.81 (m, py H-6); $^{13}C\{^1H\}$: 40.7 ppm, 41.0, 42.3 ($CH_2$), 48.6 ($CH_3OH$), 68.4 (CH), 124.5, 124.6, 124.9 (br), 142.4, 142.5, 144.7, 144.8, 154.7, 154.9 (py), 170.9, 174.2 (C=O).

### *Synthesis of the complexes*

Analytical results and colours are given in Table 1.

$Cu_2(OH)(L)\cdot nH_2O$ (L = pmg, n = 4.5; L = pmm, n = 3.5; L = lpm, n = 3.5; L = pem, n = 4.5; L = lpe, n = 4). A mixture of 10 mmol of $H_3L$ and 20 mmol (4.99 g) of copper(II) sulfate pentahydrate in 200 mL of water at 80°C was mixed with 40 mmol (1.60 g) of sodium hydroxide dissolved in an appropriate amount of water [60 mmol (2.40 g) of sodium hydroxide was used in the case of the ligand sulfates]. The hot mixture was gravitationally filtered to remove by-produced copper oxide and the filtrate was allowed to stand at room temperature to afford crystals. The crystals were collected and recrystallized by dissolving in 200 mL of hot methanol, mixing with 20 mL of water, and allowing to stand at room temperature. The pmg complex only was recrystallized from 200 mL of hot water. The complexes were obtained in a yield of 75–80%.

$Cu_2Cl(L)\cdot 4H_2O$ (L = pmg and pmm). Two mmol (1.10 g) of $Cu_2(OH)(pmg)\cdot 4.5H_2O$ was dissolved in a hot (80–90°C) mixture (150 mL) of methanol and water (2:8 in volume) and filtered. To the filtrate was added 4 mmol (298 mg) of potassium chloride dissolved in 30 mL of water and the pH of the mixture was adjusted to 5 by the addition of hydrochloric acid to precipitate crystals immediately. The crystals were collected under suction while hot and washed with water to give sky blue crystals in 80% yield. $Cu_2Cl(pmm)\cdot 4H_2O$ was prepared in this method.

$Cu_2(OAc)(L)\cdot nH_2O$ (L = pmg, n = 8; L = pmm, n = 4; L = lpm, n = 3): To a suspension of 5 mmol (2.75 g) of $Cu_2(OH)(pmg)\cdot 4.5H_2O$ in 150 mL of hot water was added 10 mmol (820 mg) of sodium acetate and the pH of the mixture was lowered to 4 by addition of acetic acid to give a clear solution. The hot solution was gravitationally filtered and upon standing crystals were obtained in 80% yield. The other two acetato complexes were similarly obtained from the corresponding hydroxo complexes.

$Cu_2(NO_2)(L)\cdot nH_2O$ (L = pmm, n = 5; L = lpm, n = 4.5). The hot aqueous solution (150 mL) containing 5 mmol (2.59 g) of $Cu_2(OH)(pmm)\cdot 3.5H_2O$ and 10 mmol (690 mg) of sodium nitrite was acidified with 10% sulfuric acid to pH = 4 and gravitationally filtered while hot. Upon standing, crystals deposited, which were recrystallized by dissolving in 100 mL of hot ethanol, filtering while hot, mixing with 20 ml of water, and allowing to stand to give the product in 75% yield. The lpm complex was prepared by this method.

$Cu_2(pz)(L)\cdot nH_2O$ (L = pmg, n = 2; L = pmm, n = 3; L = lpm, n = 3; L = pem, n = 0.5; L = lpe, n = 1). 5 mmol (2.75 g) of $Cu_2(OH)(pmg)\cdot 4.5H_2O$ and 6 mmol (408 mg) of pyrazole was dissolved in a mixture of ethanol and water (1:1 in volume) at 80°C with stirring and the hot mixture was gravitationally filtered. Upon standing for a while, crystals deposited, which were collected and dissolved in 100 mL of hot ethanol, and the solution was filtered, mixed with 20 mL of water, and allowed to stand to give the pure product. The yield was 85%. The remaining four pyrazolato complexes were prepared by a similar procedure.

$Ni_2(pz)(L)\cdot nH_2O$ (L = pmm, n = 5; L = lpm, n = 2). An aqueous solution containing 5 mmol (2.39 g) of $H_3(pmm)\cdot 1.5H_2SO_4\cdot 0.5CH_3OH$, 6 mmol (408 mg) of pyrazole, and 10 mmol (2.81 g) of nickel(II) sulfate pentahydrate at 80°C was neutralized with 30 mmol (1.20 g) of sodium hydroxide dissolved in a small amount of water to give a crystalline powder. The powder was collected and washed with water. Recrystallization was performed as follows: the powder was dissolved in 200 mL of hot ethanol, the solution was filtered, the filtrate was mixed with 40 ml of water, and the mixture was allowed to stand at room temperature to afford pure crystals in 85% yield. The lpm analogue was obtained in the same manner.

$CuNi(pz)(L)\cdot nH_2O$ (L = pmm, n = 5; L = lpm, n = 2). 2 mmol of appropriate pyrazolato copper and nickel complexes were dissolved together in 100 mL of hot ethanol and the solution was gravitationally filtered while hot. The filtrate was evaporated to 50 mL under reduced pressure. To the warmed concentrate was added 30 mL of warm water, the mixture was gravitationally filtered again, and the filtrate gave crystals upon standing in 90% yield.

### *X-ray analysis*

Slow evaporation of a solution of $Cu_2(pz)(pmm)\cdot 3H_2O$ in a mixture of methanol and water gave crystals suitable for X-ray analysis. Crystallographic data and experimental details are given in Table 6. The intensities of three representative reflections measured after every 150 reflections remained constant through the data collection. Empirical absorption corrections based on $\psi$ scans were applied. The structure was solved by the direct methods with the program SHELXS-86 [15], which gave the position of two copper atoms. The remaining non-hydrogen atoms were located by the subsequent

Table 6. Crystallographic data and experimental details

| | |
|---|---|
| Complex | $Cu_2(pz)(pmm) \cdot 3H_2O$ |
| Formula | $C_{19}H_{24}Cu_2N_6O_6$ |
| Fw | 559.53 |
| Crystal system | monoclinic |
| Space group | $P2_1/c$ (no. 14) |
| $a$ (Å) | 7.177(3) |
| $b$ (Å) | 22.605(2) |
| $c$ (Å) | 13.638(1) |
| $\beta$ (°) | 101.51(2) |
| $Z$ | 4 |
| $V$ (Å$^3$) | 2168(1) |
| $\mu$(Mo-K$\alpha$) (cm$^{-1}$) | 20.15 |
| Transm factor | 0.759–1.000 |
| Crystal color | violet |
| Crystal habit | needle |
| Crystal size (mm$^3$) | $0.2 \times 0.3 \times 0.3$ |
| $d_{calc.}$ (g/cm$^3$) | 1.71 |
| $F(000)$ | 11.44 |
| Diffractometer | Rigaku AFC-5S |
| $\lambda$(Mo-K$\alpha$) (Å) | 0.71073 |
| T (K) | 298 |
| Scan range (°) | $1.26 + 0.50 \tan\theta$ |
| Scan speed (°/min) | 4 |
| Scan mode | $\omega$-$2\theta$ |
| $2\theta_{max}$ (°) | 60 |
| Reflections measured | $0 \leqslant h \leqslant 10$ |
| | $0 \leqslant k \leqslant 32$ |
| | $-19 \leqslant l \leqslant 19$ |
| No. of reflections measured | 6950 |
| No. of reflections obsd [$\lvert Fo\rvert > 3\sigma(\lvert Fo\rvert)$] | 3754 |
| No. of parameters refined | 298 |
| $R$ | 0.053 |
| $R_w$ | 0.059 |
| $s$ | 1.83 |
| $(\Delta/\delta)_{max}$ | 0.31 |
| Largest diff peak (e/Å$^3$) | 0.73 |
| Largest diff hole (e/Å$^3$) | −1.18 |

$R = \Sigma\|Fo| - |Fc\|/\Sigma|Fo|$,
$R_w = [\Sigma w\|Fo| - |Fc\|^2/\Sigma w|Fo|^2]^{1/2}$, $w = [\sigma^2(Fo) + \{0.015(Fo)\}^2]^{-1}$.

Fourier syntheses. All the non-hydrogen atoms were refined anisotropically. Hydrogen atoms were placed at calculated positions with fixed isotropic thermal parameters equal to those of the bonded carbon atoms. The Fourier syntheses and the full-matrix least-squares refinement were carried out using the Xtal 3.2 software [16].

*Acknowledgements*—The authors thank Miss Sachiyo Nomura of Chemical Material Center, Institute for Molecular Science, Okazaki, for elemental analysis. They also express their thanks to the Institute for allowing the use of facility of X-ray diffraction measurement.

## REFERENCES

1. Zanello, P., Tamburini, S., Vigato, P. A. and Mazzocchin, G. A., *Coord. Chem. Rev.*, 1987, **77**, 165.
2. Bertoncello, K., Fallon, G. D. and Murray, K. S., *Polyhedron*, 1990, **9**, 2867.
3. Nonoyama, K., Mori, W. and Nonoyama, M., *Polyhedron*, 1994, **13**, 891.
4. Bellamy, L. J., *The Infrared Spectra of Complex Molecules*, 3rd. ed., p. 231. Chapman and Hall Ltd, London (1975).
5. Nishida, Y. and Kida, S., *Inorg. Chem.*, 1988, **27**, 447.
6. Nonoyama, M. and Yamasaki, K., *Inorg. Chim. Acta*, 1973, **7**, 676.
7. Nakamoto, K., *Infrared and Raman Spectra of Inorganic and Coordination Compounds*, 3rd. ed., p 220 and 236. John Wiley & Sons, Inc., New York (1978).
8. McKee, V., Zvagulis, M. and Reed, C. A., *Inorg. Chem.*, 1985, **24**, 2914.
9. Bürger, K.-S., Chaudhuri, P. and Wieghardt, K., *J. Chem. Soc., Dalton Trans.*, 1996, 247.
10. Kahn, O., *Molecular Magnetism*, p. 145, VCH, Weinheim (1993).

11. Handa, M., Idehara, T., Nakano, K., Kasuga, K., Mikuriya, M., Matsumoto, N., Kotera, M. and Kida, S., *Bull. Chem. Soc. Jpn*, 1992, **65,** 3241.
12. Lever, A. B. P., *Inorganic Electronic Spectroscopy*, 2nd. ed., p. 507 and 554, Elsevier, Amsterdam (1984).
13. Nonoyama, K., Ojima, H. and Nonoyama, M., *Inorg. Chim. Acta*, 1982, **59,** 275.
14. Nakao, Y., Yamashita, M., Itoh, T., Mori, W., Suzuki, S. and Sakurai, T., *Bull. Chem. Soc. Jpn.*, 1994, **67,** 260.
15. Sheldrick, G. M., *SHELX*-86, *Program for Crystal Structure Determination*, Univ. of Göttingen, Germany (1986).
16. Hall, S. R., Flack, H. D. and Stewart, J. M., *Xtal* 3.2, *Program for X-Ray Crystal Structure Analysis*, Universities of Western Australia, Geneva and Maryland (1992).